Journal of Catalysis **207,** 37–45 (2002)
doi:10.1006/jcat.2002.3529, available online at http://www.idealibrary.com on IDEAL®

Hydrogenation of Nitrate in Water to Nitrogen over Pd–Cu Supported on Active Carbon

Yusuke Yoshinaga, Tomonobu Akita, Ikko Mikami, and Toshio Okuhara[1]

Graduate School of Environmental Earth Science, Hokkaido University, Sapporo 060-0810, Japan
E-mail: oku@ees.hokudai.ac.jp

Received August 20, 2001; revised December 28, 2001; accepted December 28, 2001

Catalytic removal of nitrate in water by hydrogenation was investigated by using supported Pd–Cu catalysts at 333 K in a flow system. Active carbon (AC) was superior in conversion, selectivity, and insolubility to other supports. Pd and Cu were not dissolved when supported on AC, even at low pH reaction conditions, while they were considerably released from the surface of γ-Al_2O_3, SiO_2, and ZrO_2. The contact time dependence of the reactant and products suggested that the hydrogenation of NO_3^- is a consecutive reaction with NO_2^- as an intermediate product and that the hydrogenation of NO_2^- is a key step in determining selectivity to N_2 and NH_3. The conversion of NO_3^- was enhanced greatly by the addition of a small amount of Cu to 5 wt% Pd/AC or of Pd to 3 wt% Cu/AC, indicating that the Pd–Cu site was indispensable to activate the nitrate ion. The yield of N_2 went through a maximum at 0.6 wt% Cu in the 5 wt% Pd–Cu/AC. A similar dependence of the N_2 yield on Cu content for NO_2^- hydrogenation strongly supports the proposed reaction pathways. The enhancement of N_2 selectivity by the addition of small amounts of Cu can be explained by the selective poisoning of the edge or corner sites of the Pd particles by Cu atoms.

Key Words: **hydrogenation of nitrate; nitrite; Pd–Cu; active carbon; nitrogen.**

INTRODUCTION

Harmful nitrogen-containing compounds such as ammonia, nitrate, and nitrite become aggravated in ground water (1). The sources of these compounds are fertilizers, animal excretion, and industrial effluents (2). Nitrate (NO_3^-) brings about eutrophication of rivers and lakes. In addition, NO_3^- is reduced to nitrite (NO_2^-) in the human body, which is responsible for the blue-baby syndrome and possibly a precursor of carcinogenic nitroso amine (3).

The European community has set the maximum levels of nitrate and nitrite concentrations in drinking water at 50 mg of nitrate $\cdot$ dm^{-3} (corresponding to 50 ppm) and 0.1 mg of nitrite $\cdot$ dm^{-3} (0.1 ppm). In addition, the World Health Organization has proposed 25 mg of nitrate $\cdot$ dm^{-3} as a guide level for drinking water. In Japan, the total concentration of nitrate and nitrite in ground water is limited to 10 mg of N-atoms $\cdot$ dm^{-3} (corresponding to 44 ppm of NO_3^-) in the *Notification of the Ministry of Environment in 1999*.

As current practical technologies for the removal of nitrate from water, physicochemical and biological processes have been utilized (4, 5). An ion-exchange method using anion-exchange resins is one of the physicochemical processes, but regeneration of the resins is required for reuse. Moreover, ion-exchange resins that are selective for nitrate have not been fully developed yet. While reverse osmosis and electrodialysis are also physicochemical processes, they are separation processes that do not transform nitrate to harmless compounds. Biological denitrification is recognized as a useful method for the selective conversion of nitrate into harmless gaseous nitrogen. However, this process has the disadvantage of producing undesirable by-products such as NO_2^-, NO, NO_2, and N_2O. In addition, it is necessary to precisely control the concentration of NO_3^- and pH value in this method.

Catalytic hydrogenation of nitrate to nitrogen with H_2 over solid catalysts has attracted much attention as a new technology. The hydrogenation of nitrate using Pd bimetallic catalysts has extensively been studied (5–17) since the discovery of a palladium–copper bimetallic catalyst by Vorlop and Tacke in 1989 (18).

Vorlop and coworkers (5, 6) claimed that bimetallic Pd catalysts were active for the hydrogenation of NO_3^-, while a monometallic Pd catalyst was inactive. Thereafter, Pintar *et al.* (7, 8) examined the effect of the countercation of nitrate on the nitrate hydrogenation over Pd–Cu/Al_2O_3 and found that the rate constant increased in the order $K^+ < Na^+ < Ca^{2+} < Mg^{2+} < Al^{3+}$ (7, 8). Then Strukul *et al.* (9) reported a highly active and selective Pd–Cu/Al_2O_3 catalyst obtained by a cogelation method. Deganello *et al.* (10) showed that pumice-supported Pd–Cu obtained from palladium acetyl acetonate and Cu acetyl acetonate was more active than that from $Pd(NH_3)_4(NO_3)_2$ and $Cu(NO_3)_2$. Ilinitch *et al.* (11) pointed out that the hydrogenation of NO_3^- is a consecutive reaction through NO_2^- and NO. More recently, Prüsse *et al.* inferred from their results that Pd–Sn/Al_2O_3 was more active than Pd–Cu/Al_2O_3

[1] To whom correspondence should be addressed. Fax: 81-11-706-4513.

0021-9517/02 $35.00

(12, 13) and proposed a mechanistic model for reaction (14). Strukul *et al*. (15) showed further that Pd–Sn/ZrO_2 was highly selective to N_2 as compared with Pd–Sn/Al_2O_3. Pintar *et al*. (16, 17) tried to combine an ion-exchange system with a Pd–Cu/Al_2O_3 catalyst for removal of NO_3^-. Matatov-Meytal *et al*. (19) claimed glass fibers in the form of woven cloth as a new type support. Hayashi *et al*. (20) examined the influence of the addition of Cu to a commercial Pd/active carbon catalyst on activity and selectivity.

While many studies were performed as described above, the most suitable support for Pd–Cu has not been revealed yet. The present study aims to investigate which support gives high activity, selectivity, and stability for hydrogenation of nitrate in water with hydrogen over supported Pd–Cu. Stability was evaluated from the amount of Pd and Cu dissolved into the aqueous solution during the reaction, since considerable amounts of dissolved metals from some catalysts were detected during the reaction. Then we examined systematically the effects of Cu and Pd content on stationary catalytic activity and selectivity by using a liquid–gas flow system. To compare catalytic activity accurately, it was determined from the conversion–contact time dependence. Selectivity to N_2 for NO_3^- hydrogenation was evaluated at 100% conversion of NO_3^-, because selectivity became constant independent of the contact time at 100% conversion. Influences of Cu content on activities and selectivities for NO_3^- and NO_2^- hydrogenations are discussed on the basis of the microstructure of the Pd–Cu bimetallic particles characterized mainly by X-ray diffraction (XRD).

EXPERIMENTAL

Catalysts

As a support, active carbon (AC) was purchased from Wako Pure Chem. Ind. Ltd. (1155 $m^2 \cdot g^{-1}$). ZrO_2 (68 $m^2 \cdot g^{-1}$) was obtained by the calcination of Zr hydroxide (Daiichi Kigenso Kagaku Kogyo Co., Ltd.) at 723 K. SiO_2 (Aerosil 300, 274 $m^2 \cdot g^{-1}$), γ-Al_2O_3 (JRC-ALO-4, 166 $m^2 \cdot g^{-1}$), and TiO_2 (Aerosil P-25, 46 $m^2 \cdot g^{-1}$) were also used as support. The Pd–Cu catalysts were prepared by an incipient wetness method using $PdCl_2$ (Wako Pure Chem. Ind. Ltd.) and $Cu(NO_3)_2$ (Wako Pure Chem. Ind. Ltd.). An aqueous solution of 1.13×10^{-4} mol $\cdot$ cm^{-3} of $PdCl_2$ was added dropwise to a support at room temperature. After drying at 373 K for 12 h, the aqueous solution of $Cu(NO_3)_2$ (1.66×10^{-4} mol $\cdot$ cm^{-3}) was introduced at room temperature to the solid. Again the resulting wet–solid was dried at 373 K for 12 h. In the case of the AC support, Pd and Cu contents were varied from 0 to 5 and 0 to 3 wt%, respectively. For the other supports, the loadings were 5 wt% Pd and 0.6 wt% Cu. In addition, a physical mixture of the monometallic 5 wt% Pd/AC and 3 wt% Cu/AC was used as catalyst. Pd–Cu/AC was pretreated in a flow of He at 573 K for 1 h and then in a flow of H_2 at 573 K for 2 h. The other supported Pd–Cu catalysts were pretreated in a flow of H_2 at 723 K for 2 h.

Catalytic Reactions

The hydrogenation of nitrate with H_2 was performed in a gas–liquid flow reactor (Pyrex tube, 10-mm inside diameter). Hydrogen gas and the aqueous solution were well mixed by passing through a glass filter just before the catalyst bed. The catalyst powder was fixed in the glass reactor by using glass wool. The reactor was maintained at 333 K in a water bath. An aqueous solution of 200 ppm NO_3^- or NO_2^- and H_2 was fed into the reactor under atmospheric pressure through a preheated zone (Pyrex tube, 4-mm inside diameter). The flow rate of the liquid was varied from 12.6 to 132 $cm^3 \cdot h^{-1}$ (41–430 μmol of $NO_3^- \cdot h^{-1}$) and that of H_2 was adjusted to 84 $cm^3 \cdot h^{-1}$ (3.5 mmol $\cdot$ h^{-1}). The aqueous solution of NO_3^- was prepared from $NaNO_3$ (Wako Pure Chem. Ind. Ltd.) or HNO_3 (Wako Pure Chem. Ind. Ltd.) at pH values of 5.4 and 2.3, respectively. The solution of NO_2^- was prepared from $NaNO_2$ (Wako Pure Chem. Ind. Ltd.) at a pH value of 5.4. The gas at the outlet of the reactor was sampled with a microsyringe and analyzed by gas chromatography with columns of Molecular Sieves 5A (for N_2 and O_2) and Porapak Q (for N_2O). The concentrations of NH_3, NO_2^-, and NO_3^- in the aqueous phase were analyzed quantitatively using a flow injection analysis system (consisting of a Soma Optics S-3250 detector and a Sanuki Industry FI-710 analyzer equipped with a RX-703T pump and a R-5000C reactor). The solution was diluted with water for analysis of NO_2^- and NO_3^- and was used directly for NH_3. In these measurements, the detection limits of NO_3^-, NO_2^-, and NH_4^+ were 0.001, 0.001, and 0.1 ppm, respectively.

Other Measurements

X-ray diffraction patterns of Pd–Cu/AC were recorded with an X-ray diffractometer (Rigaku, Mini Flex). The catalyst powder, which was dried at about 333 K, was pressed on a glass holder at room temperature and was set in the diffractometer. The crystallite size of the Pd particles was calculated from the half width of the diffraction peak ($2\theta = 40.1^\circ$) using Scherrer equation, $D = 0.9\lambda/\beta \cos\theta$, where λ is the X-ray wavelength (Cu$K\alpha$), θ is the diffraction angle, and β is the line width. The dissolved amounts of Pd and Cu were measured using inductively coupled plasma (Shimadzu ICPS-7000) and using the effluent solution directly.

RESULTS

Effect of Support and pH on Hydrogenation of NO_3^-

Table 1 shows the conversion and selectivity for nitrate hydrogenation over various supported Pd–Cu catalysts

TABLE 1

Effects of Support for Pd–Cu Catalyst and pH Value of Reactant Solution

Catalyst[a]	Surface area ($m^2\ g^{-1}$)	pH[b] Inlet	pH[b] Outlet	Conversion[c] (%)	Selectivity[d] (%) N_2	NO_2^-	NH_3	N_2O	Dissolved amount[e] (%) Pd	Cu
Pd–Cu/SiO_2	278	5.4	10.0	95.5	11.6	11.2	77.2	0.0	3.94	10.6
Pd–Cu/Al_2O_3	100	5.4	—	45.7	56.9	30.5	4.7	7.9	0.01	6.3
Pd–Cu/ZrO_2	68	5.4	11.1	84.5	40.4	14.6	45.0	0.0	1.37[f]	26.0[f]
Pd–Cu/AC	1155	5.4	11.2	97.1	78.3	0.3	21.4	0.0	0.00	0.1[g]
Pd–Cu/Al_2O_3	100	2.3	3.5	56.9	45.4	0.0	54.6	0.0	0.00[h]	30.7[h]
Pd–Cu/AC	1155	2.3	—	99.9	86.8	0.1	13.1	0.0	0.01	0.1[g]

[a] Pd, 5.0 wt%, Cu, 0.6 wt% (Pd/Cu atomic ratio = 5).
[b] pH 5.4 and 2.3 for $NaNO_3$ and HNO_3, respectively.
[c] Reaction conditions: NO_3^-, 200 ppm (3.22 mmol · dm^{-3}), 39 $cm^3 \cdot h^{-1}$; H_2 (1 atm), 84 $cm^3 \cdot h^{-1}$; catalyst, 1.0 g; reaction temperature, 333 K; reaction time, 6 h.
[d] On the basis of *N* atoms.
[e] Percentage of the amount of metal detected in the solution at the outlet vs that in the fresh catalyst.
[f] Only in the initial stage (1 h) were the dissolutions detected.
[g] Within the experimental error.
[h] 3.7% Al was dissolved.

after 6 h. The dissolved amounts of Pd and Cu during the reaction are also summarized in Table 1, where they are expressed as percentages of the total amount of metal atom. Table 1 demonstrates that AC gave a high conversion of nitrate (97.1%) and a high selectivity to N_2 (78.3%) in the hydrogenation of NO_3^- (from $NaNO_3$) under these reaction conditions. The dissolved amounts of Pd and Cu from 5 wt% Pd to 0.6 wt% Cu/AC were negligibly small. When the solution of HNO_3 (pH 2.3) was used over 5 wt% Pd–0.6 wt% Cu/AC, both the conversion and the selectivity became higher. Again, no dissolution of Pd and Cu was detected in this reaction. However, in the cases of SiO_2 and ZrO_2, Pd and Cu were considerably dissolved. It addition, besides the metals, Al was released in the solution under the acidic conditions from Pd–Cu/Al_2O_3 (Table 1).

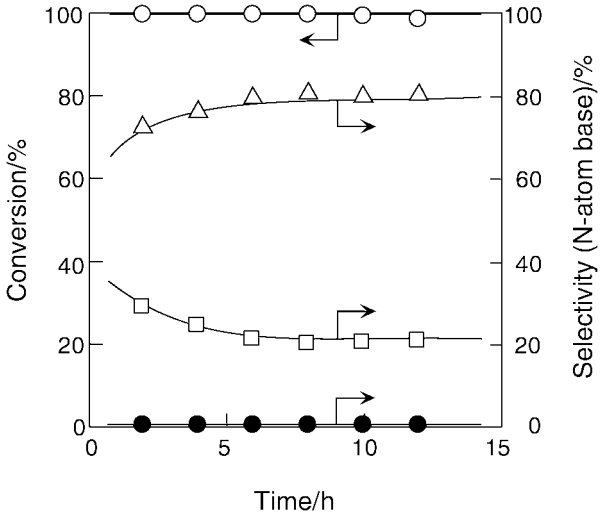

FIG. 1. Time course of hydrogenation of nitrate over 5 wt% Pd–0.6 wt% Cu/AC: (○) NO_3^-, (●) NO_2^-, (△) N_2, and (□) NH_3. Reaction conditions: catalyst weight, 1.0 g; temperature, 333 K; reactant, NO_3^- (200 ppm from $NaNO_3$), 0.13 mmol · h^{-1}; H_2 (1 atm), 3.5 mmol · h^{-1}; weight hourly space velocity (WHSV) = 39 h^{-1}.

In Fig. 1, a typical time course for the catalytic hydrogenation of nitrate over 5 wt% Pd–0.6 wt% Cu/AC is given. Under these conditions, the conversion was 100% for at least 12 h. While the selectivity changed at the initial stage of reaction, the selectivity to N_2 or NH_3 became constant after about 5 h. The amounts of N_2O and NO_2^- formed were negligibly small. The amount of reacted NO_3^- for 12 h was about 3 and 15 times higher than the amounts of Pd and Cu atoms present initially in the catalyst, respectively. This indicates that the reaction proceeded catalytically.

Figure 2 presents the dependence of contact time over 5 wt% Pd–3 wt% Cu/AC, where the contact time is shown by W/F (W = catalyst weight and F = flow rate of the aqueous solution of NO_3^-). With the decrease in NO_3^-, NO_2^- appeared at short contact times. As the contact time increased further, the composition of NO_2^- decreased rapidly through a maximum value. N_2 was formed in parallel with NH_3 at all contact times.

Effects of Pd and Cu Loadings on Activity and Selectivity

Table 2 compares the activities between 5 wt% Pd–3 wt% Cu/AC and monometallic catalysts for the NO_3^- hydrogenation. While 5 wt% Pd–3 wt% Cu/AC gave 100% conversion, the conversions over 5 wt% Pd/AC and 3 wt% Cu/AC were only 2.7 and 3.2%, respectively, indicating that the coexistence of Pd and Cu is indispensable for the hydrogenation of NO_3^-. A physical mixture of 5 wt% Pd/AC and 3 wt% Cu/AC showed a conversion of 53.2% (Table 2). Probably not only contact between the catalyst particles but also

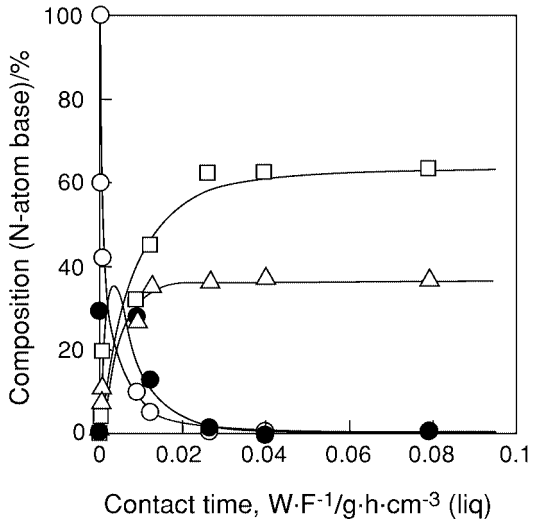

FIG. 2. Contact time dependence of the hydrogenation of nitrate over 5 wt% Pd–3 wt% Cu/AC: (○) NO_3^-, (●) NO_2^-, (△) N_2, and (□) NH_3. Reaction conditions: catalyst weight, 0.05–1.0 g; temperature, 333 K; reactant, NO_3^- (200 ppm from $NaNO_3$), 0.04–0.43 mmol · h^{-1}; H_2 (1 atm), 3.5 mmol · h^{-1}.

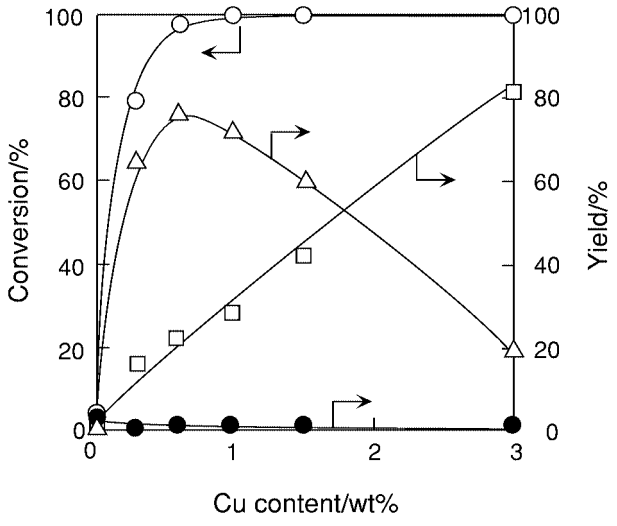

FIG. 3. Effects of Cu content on conversion and yield of products in the hydrogenation of nitrate over 5 wt% Pd–Cu/AC: (○) NO_3^-, (●) NO_2^-, (△) N_2, and (□) NH_3. Reaction conditions: catalyst weight, 1.0 g; temperature, 333 K; NO_3^- (200 ppm from $NaNO_3$), 0.13 mmol · h^{-1}; H_2 (1 atm), 3.5 mmol · h^{-1}; WHSV = 39 h^{-1}.

hydrogen spillover through the catalyst particles brought about the activity.

Figure 3 shows the influences of the Cu content of 5 wt% Pd–Cu/AC on the conversion and yields of N_2 and NH_3 (the yield is defined as the product of conversion and selectivity). The conversion of NO_3^- was greatly enhanced by the addition of small amounts of Cu to 5 wt% Pd/AC. While the yield of NH_3 increased monotonically, the yield of N_2 first increased as the Cu content increased and then decreased through a maximum at 0.6 wt% Cu.

Figure 4 presents the effects of the Pd content of Pd–0.6 wt% Cu/AC on the conversion of NO_3^- and yields of N_2 and NH_3. The addition of only 0.1% Pd enhanced the conversion significantly, and further addition brought about 100% conversion. An appreciable amount of NO_2^- was detected at the 0.1 wt% Pd. The yield of N_2 increased as Pd content increased.

In Fig. 5, changes in the reaction rate and N_2 selectivity as a function of the Cu content of 5 wt% Pd–Cu/AC are shown, where the reaction rate was evaluated from the W/F dependence of the conversion, and the selectivity to N_2 was measured at 100% NO_3^- conversion. As described above, selectivity was constant at 100% conversion independent of the contact time. The reaction rate increased effectively as the Cu content increased to 1.5 wt% and became nearly constant above 1.5 wt% Cu.

Hydrogenation of NO_2^-

The results of Fig. 2 suggest that the hydrogenation of NO_3^- is a consecutive reaction through NO_2^- as an intermediate product. Thus the step of NO_2^- hydrogenation is critical for selectivity. The W/F dependence of the composition over 5 wt% Pd–0.6 wt% Cu/AC is given in Fig. 6.

TABLE 2

Hydrogenation of Nitrate over AC-Supported Catalysts

Catalyst	Pd loading (wt%)	Cu loading (wt%)	Conversion[a] (%)	Selectivity[b] (%)			
				N_2	NO_2^-	NH_3	N_2O
Pd–Cu/AC	5.0	3.0	100	18.3	0.0	81.7	0.0
Pd/AC	5.0	0	2.7	15.9	12.7	71.4	0.0
Cu/AC	0	3.0	2.2	16.4	74.6	9.0	0.0
Pd/AC + Cu/AC (1 : 1)	5.0	3.0	53.2	47.8	30.5	21.7	0.0

[a] Reaction conditions: NO_3^-, 200 ppm (3.22 mmol · dm^{-3}), 39 cm^3 · h^{-1}; H_2 (1 atm), 84 cm^3 · h^{-1}; catalyst, 1.0 g; reaction temperature, 333 K; reaction time, 6 h.

[b] On the basis of *N* atoms.

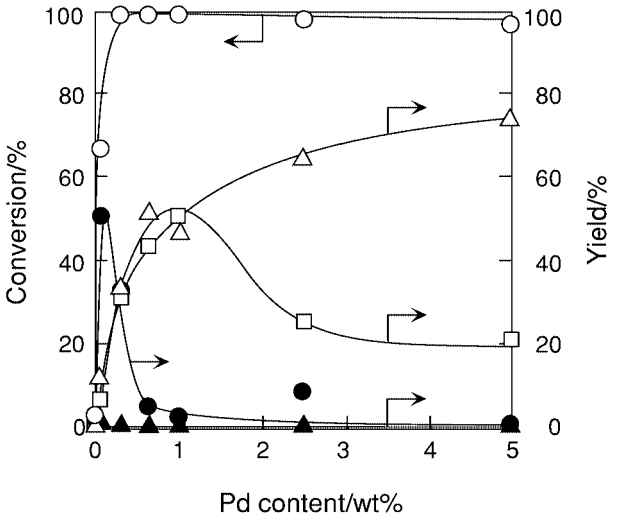

FIG. 4. Effects of Pd content on conversion and yield of products in the hydrogenation of nitrate over Pd–0.6 wt% Cu/AC: (○) NO_3^-, (●) NO_2^-, (△) N_2, (▲) N_2O, and (□) NH_3. Reaction conditions: catalyst weight, 1.0 g; temperature, 333 K; reactant, NO_3^- (200 ppm from $NaNO_3$), 0.13 mmol · h^{-1}; H_2 (1 atm), 3.5 mmol · h^{-1}, WHSV = 39 h^{-1}.

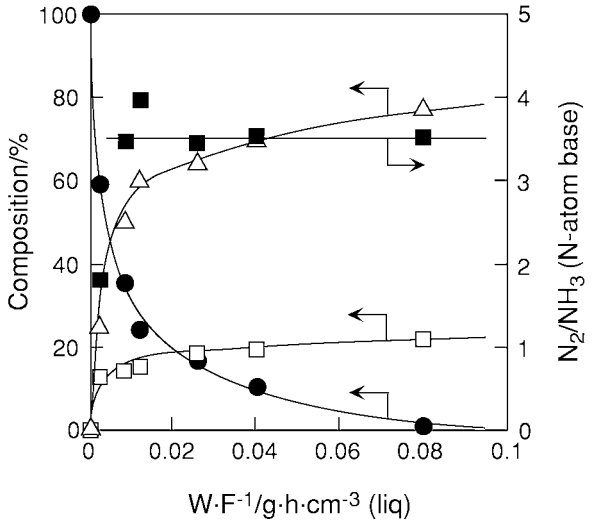

FIG. 6. W/F-dependence of the compositions of NO_2^- (●), N_2 (△), and NH_3 (□) in hydrogenation of nitrite over 5 wt% Pd–0.6 wt% Cu/AC: (■) ratio of the amount of N_2 to that of NH_3 on the basis of N atoms. Reaction conditions: catalyst weight, 0.1–1.0 g; temperature, 333 K; reactant, NO_2^- (200 ppm from $NaNO_3$), 0.05–0.57 mmol · h^{-1}; H_2 (1 atm), 3.5 mmol · h^{-1}.

As W/F increased, the NO_2^- decreased rapidly, and N_2 and NH_3 appeared with a constant ratio.

Figure 7 presents the reaction rate and selectivity to N_2 for the NO_2^- hydrogenation as a function of the Cu content of 5 wt% Pd–Cu/AC. Contrary to the hydrogenation of NO_3^- (Fig. 5), the hydrogenation of NO_2^- proceeded rapidly without Cu. Upon the addition of Cu, the reaction rate increased slightly. As is not shown in Fig. 7, the monometallic 3 wt% Cu/AC catalyst was inactive for NO_2^- hydrogenation. Selectivity to N_2 was enhanced from 40% (without Cu) to about 80% by the addition of 0.3–1.0 wt% Cu. Further addition of Cu caused a decrease in N_2 selectivity. It is worth noting that the change in selectivity was similar to that of the change in NO_3^- hydrogenation (Fig. 5).

Since the monometallic 5 wt% Pd/AC catalyst was highly active for the hydrogenation of NO_2^-, the effects of Pd loading of Pd/AC were examined. As summarized in Table 3,

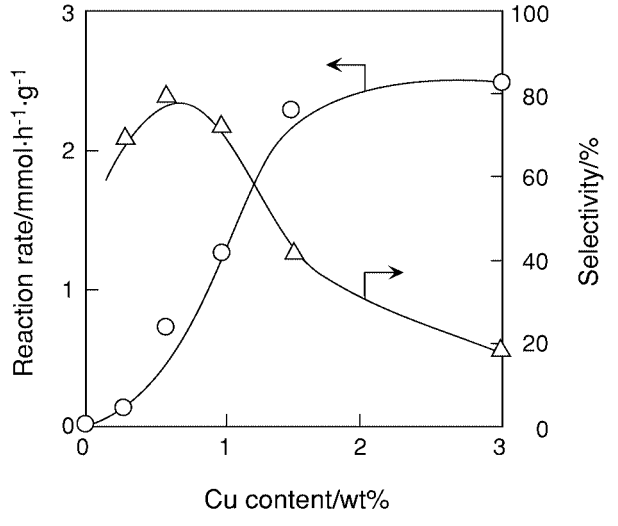

FIG. 5. Changes in reaction rate (○) and N_2 selectivity (△) as a function of the Cu content in the hydrogenation of nitrate over 5 wt% Pd–Cu/AC. Reaction conditions: catalyst weight, 1.0 g; Pd, 5.0 wt%; temperature, 333 K; reactant, NO_3^- (200 ppm from $NaNO_3$), 0.04–0.17 mmol · h^{-1}; H_2 (1 atm), 3.5 mmol · h^{-1}.

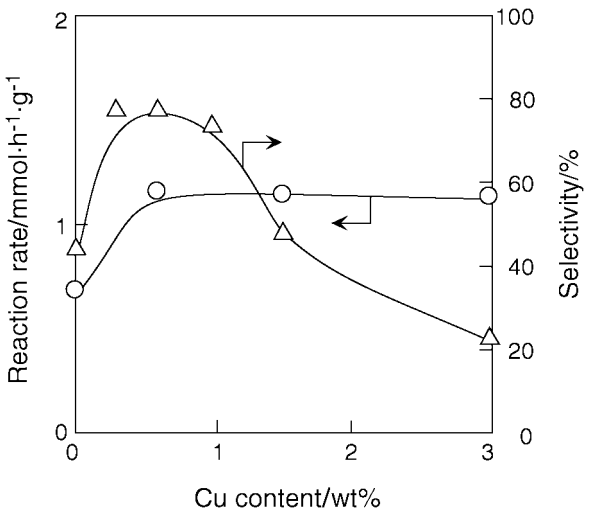

FIG. 7. Changes in reaction rate (○) and N_2 selectivity (△) as a function of the Cu content in hydrogenation of nitrite over 5 wt% Pd–Cu/AC. Reaction conditions: catalyst weight, 1.0 g; temperature, 333 K; reactant, NO_2^- (200 ppm from $NaNO_3$), 0.05–0.17 mmol · h^{-1}; H_2 (1 atm), 3.5 mmol · h^{-1}.

TABLE 3

Effects of Loading Amount of Pd on Conversion and Selectivity for Hydrogenation of Nitrite

Catalyst	Pd loading (wt%)	Pd crystallite size[a] (nm)	Conversion[b] (%)	Selectivity[c] (%)		
				N_2	NH_3	N_2O
Pd/AC	5.0	6.7	91.2	55.8	44.2	0.0
Pd/AC	2.5	6.0	86.5	48.1	51.9	0.0
Pd/AC	1.0	—	53.6	41.3	58.7	0.0
Pd/AC	0.6	—	35.6	30.0	70.0	0.0

[a] Calculated using Scherrer equation from Pd(111) diffraction.

[b] Reaction conditions: NO_2^-, 200 ppm (4.34 mmol · dm^{-3}), 39 $cm^3 \cdot h^{-1}$; H_2 (1 atm), 84 $cm^3 \cdot h^{-1}$; catalyst, 1.0 g; reaction temperature, 333 K; reaction time, 6 h.

[c] On the basis of *N* atoms.

both the conversion and N_2 selectivity increased monotonically as the Pd loadings increased. As also shown in Table 3, the crystallite size estimated from the XRD peaks became larger as the Pd loadings increased and was about 6.6 nm at 5 wt% Pd (Table 3).

XRD Patterns of Pd–Cu/AC

Figure 8 illustrates the XRD patterns of Pd/AC, Cu/AC, and Pd–Cu/AC. While the monometallic 3 wt% Cu/AC catalyst gave sharp peaks due to the Cu crystallites (Fig. 8g), 5 wt% Pd–Cu/AC (Fig. 8f) did not show the peaks of Cu crystallites at Cu loading levels of 0.3–5 wt%. Contrary to the Cu crystallites, the peaks due to Pd crystallites appeared for all 5 wt% Pd–Cu/AC catalysts. The half-widths of the XRD peaks of Pd were almost independent of the Cu content for 5 wt% Pd–Cu/AC except for the sample of 5 wt% Pd–3 wt% Cu/AC sample. As shown in Table 4, the crystallite size of Pd was determined to be 15.4 nm for 5 wt% Pd–3 wt% Cu/AC, while those for the other Pd–Cu/AC catalysts were 11.0–12.0 nm.

Pd–Cu bimetallic phases were detected above 1.0 wt% Cu. A CuPd phase (21) was detected at $2\theta = 43$, 62, and 79 at 1.5 wt% Cu, and a Pd_3Cu phase (22) was observed at 3 wt% Cu (Figs. 8e and f). Table 4 also shows the conversion of NO_3^- and the selectivity to N_2 for 5 wt% Pd–Cu/AC. N_2 selectivity decreased significantly as the Cu content increased, while the size of the Pd crystallites remained almost unchanged.

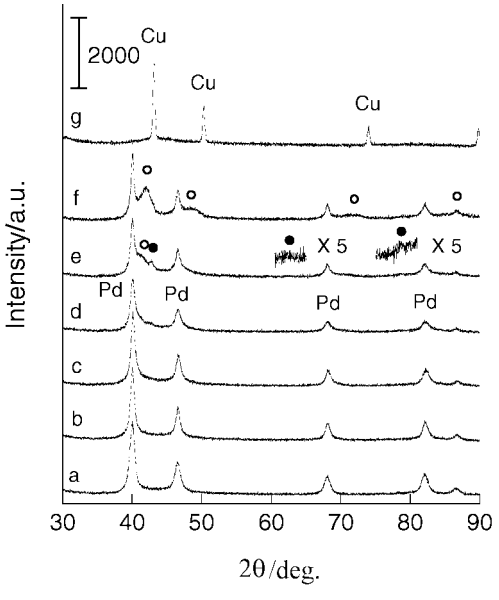

FIG. 8. XRD patterns of 5 wt% Pd–Cu/AC and 3 wt% Cu/AC: (●) CuPd and (○) Cu_3Pd: (a) 5 wt% Pd/AC, (b) 5 wt% Pd–0.3 wt% Cu/AC, (c) 5 wt% Pd–0.6 wt% Cu/AC, (d) 5 wt% Pd–1 wt% Cu/AC, (e) 5 wt% Pd–1.5 wt% Cu/AC, (f) 5 wt% Pd–3 wt% Cu/AC, and (g) 3 wt% Cu/AC.

DISCUSSION

Effects of Support

The discovery by Vorlop and coworkers (5) of the Pd–Cu bimetallic catalyst stimulated research of the hydrogenation of nitrate in water. Various supports for Pd bimetallic catalyst have been examined. γ-Al_2O_3 deserves our attention, since many researchers have utilized this support. In addition, it was claimed that ZrO_2 is superior in activity to γ-Al_2O_3 (15). Considering these conditions, we first attempted to determine the most suitable support for a Pd–Cu catalyst for the hydrogenation of nitrate.

Table 1 shows that the supports with high surface areas, such as AC and SiO_2, brought about high conversions for the hydrogenation of NO_3^-. However, in the case of Pd–Cu/SiO_2, the reactant solution became yellow after the reaction, showing a considerable amounts of Pd and Cu dissolved during the reaction (Table 1). When Pd–Cu/γ-Al_2O_3 was used at pH 2.3, not only Cu but also γ-Al_2O_3 itself dissolved (Table 1). This result is consistent with that of Pintar *et al.* (7, 8). Table 1 further demonstrates that both Pd and Cu were released from Pd–Cu/ZrO_2, while ZrO_2 itself was stable. In contrast to these supports, AC was excellent for Pd–Cu, since it not only showed the high activity and selectivity to N_2 but also the insolubility of the metallic

TABLE 4

Effects of Loading Amount of Cu on Conversion and Selectivity for Hydrogenation of Nitrate

Catalyst[a]	Cu loading (wt%)	Pd crystallite size[b] (nm)	Conversion[c] (%)	Selectivity[d] (%)			
				N_2	NO_2^-	NH_3	N_2O
Pd–Cu/AC	0	9.5	2.7	15.9	12.7	71.4	0
Pd–Cu/AC	0.3	12.1	78.9	81.5	0	18.5	0
Pd–Cu/AC	0.6	11.7	97.1	78.3	0.3	21.4	0
Pd–Cu/AC	1.0	11.0	99.2	71.7	0.9	27.4	0
Pd–Cu/AC	1.5	11.3	99.9	40.9	0	59.1	0
Pd–Cu/AC	3.0	15.4	100	18.3	0	81.7	0

[a] Pd, 5.0 wt%.

[b] Calculated using Scherrer equation from Pd(111) diffraction.

[c] Reaction conditions: NO_3^-, 200 ppm (3.22 mmol · dm^{-3}), 39 $cm^3 \cdot h^{-1}$; H_2 (1 atm), 84 $cm^3 \cdot h^{-1}$; catalyst, 1.0 g; reaction temperature, 333 K; reaction time, 6 h.

[d] On the basis of *N* atoms.

components (Table 1). These findings are first reported in the present study.

Hörold *et al.* (5) and Prüsse *et al.* (12) pointed out that selectivity to N_2 depends on the pH of the reactant solution. They claimed that selectivity to N_2 increased as the pH value decreased in the NO_3^- hydrogenation over Pd–Cu/γAl_2O_3 (5, 12). This trend was also observed for Pd–Cu/AC in the present study (Table 1). Table 1 demonstrates that Pd–Cu/AC was stable even at a low pH. Thus we chose AC as the support for a Pd–Cu bimetallic catalyst for further study.

Reaction Pathways

The dependence of contact time (Fig. 2) indicates that NO_2^- is the intermediate in the consecutive reaction of NO_3^- hydrogenation. As a matter of fact, NO_2^- hydrogenation produced N_2 and NH_3 concurrently over Pd–Cu/AC, supporting the above idea. In other words, selectivity in NO_3^- hydrogenation would be essentially governed by NO_2^- hydrogenation. The similarity of the selectivity change on Cu content between the hydrogenation of NO_3^- (Fig. 5) and that of NO_2^- (Fig. 7) is consistent with the proposed reaction pathways.

The proposed scheme is shown in Eq. [1].

$$NO_3^- \xrightarrow{H_2} NO_2^- \begin{cases} \xrightarrow{H_2} N_2 \\ \xrightarrow{H_2} NH_3 \end{cases} \qquad [1]$$

Since the bimetallic sites of Pd and Cu are indispensable for the acceleration of NO_3^- hydrogenation, NO_3^- would be activated on Pd–Cu sites to form NO_2^-. The hydrogenation of NO_2^- took place readily on both Pd sites and Pd–Cu sites (Fig. 7).

Roles of Pd–Cu Bimetallic Sites and Pd Sites

XRD patterns of Pd–Cu/AC (Fig. 8) revealed that the microstructures of the metallic particles greatly changed depending on the loading of Cu in 5 wt% Pd–Cu/AC. The fact that 3 wt% Cu/AC gave sharp peaks of Cu crystallites, but that no Cu peak was detected for Pd–Cu/AC, indicates that Cu interacted strongly with the Pd particles to form Pd–Cu particles on AC. Van Langeveld *et al.* (23) reported that by using atomic emission spectroscopy, Cu was enriched on the top surface layer of a Pd–Cu film prepared by a deposition method. Furthermore, Rochefort *et al.* (24) determined by LEIS that the surface composition of the (111) surface of a Pd50Cu50 single crystal was Pd45Cu55. On the other hand, Renouprez *et al.* (21) analyzed a Pd–Cu/SiO_2 catalyst prepared from acetyl acetonate complexes by LEIS and concluded that when treated at 670 K in He, Cu covered the Pd particles. Since only Pd peaks were detected at a Cu content up to 0.6 wt% (Fig. 8) in the present study, we can presume that Cu atoms were located at the surface of the Pd crystallites for Pd–Cu/AC with these Cu contents.

New peaks due to Pd–Cu alloys appeared when the Cu loading exceeded 1.5 wt% for 5 wt% Pd–Cu/AC. Cu_3Pd (cubic and tetragonal) and CuPd (cubic) are known as crystallite phases of Pd–Cu bimetals (21, 22, 25, 26). As Fig. 8 shows, the CuPd (1 : 1) phase was detected at $2\theta = 43$, 62, and 79° for 5 wt% Pd–1.5 wt% Cu/AC. In addition, the peaks at 42, 48, 68, and 82° assignable to Cu_3Pd were observed for 5 wt% Pd–3 wt% Cu/AC. These Pd–Cu phases as well as Pd crystallites were copresent at Cu loadings higher than 1.5 wt% (Fig. 8). From these XRD patterns, models of metallic particles can be proposed, as shown in Fig. 9.

As described above, selectivity in NO_3^- hydrogenation would be governed at the step of NO_2^- hydrogenation. Since Pd gave high activity for the hydrogenation of NO_2^-, the effects of Pd particle size should be considered. As the loading amount of Pd for Pd/AC increased (the

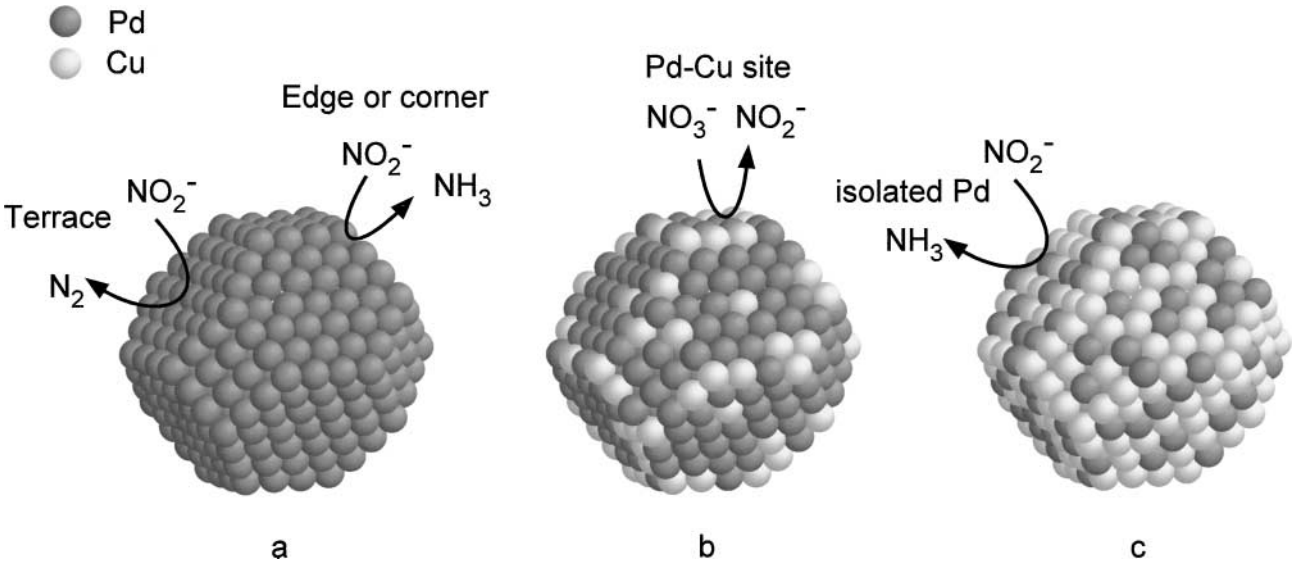

FIG. 9. Proposed models of Pd and Pd–Cu particles: (a) 5 wt% Pd, (b) 5 wt% Pd–0.6 wt% Cu, (c) 5 wt% Pd–3 wt% Cu.

crystallite size also increased), the selectivity to N_2 was enhanced (Table 3). This trend can be understood in terms of structure-sensitivity (27). There are various kinds of Pd sites with different coordinative unsaturation at the surface of Pd particles and these exhibit different selectivities for hydrogenation. Since edge and corner sites of Pd in Pd microcrystallites possess high abilities for hydrogenation (28), these sites are probably favorable for deep hydrogenation of NO_2^-, that is, formation of NH_3. On the other hand, N_2 would be favorably formed on the terrace sites of the Pd crystallites, because these sites have mild hydrogenation abilities. This presumption is consistent with the selectivity change on Pd particle size (Table 3).

It should be emphasized that the addition of Cu at less than 1 wt% greatly enhanced the selectivity to N_2 for hydrogenation of both NO_3^- and NO_2^- (Figs. 3 and 7). If the NO_2^- hydrogenation step is critical for selectivity, Pd sites as well as Pd–Cu sites may play an important role. The addition of Cu had only a minor effect on the rate of NO_2^- hydrogenation and the monometallic Cu/AC was inactive for NO_2^- hydrogenation. These results are in accordance with the above idea. Ilinitch *et al.* (11) inferred from their results that the reaction rate of NO_2^- hydrogenation increased the amount of Cu for 5 wt% Pd–Cu/Al_2O_3. On the other hand, Prüsse and Vorlop observed that the hydrogenation activity of nitrate decreased on the addition of Cu to Pd/Al_2O_3; they claimed that the sites for hydrogenation are Pd but not Pd–Cu (14). The different effects of Cu on the Pd catalysts were probably brought about by the difference in support and preparation method.

The location of the Cu atoms on the Pd particles would relate closely to the selectivity change, as is discussed below. Mélendrez *et al.* (28) observed that the addition of Cu to Pd/SiO_2 decreased the CO adsorption on Pd sites with low coordinative unsaturation. They concluded that Cu atoms were deposited on Pd edge and corner sites. If Cu atoms are deposited on the edge or corner sites of Pd in the Pd–Cu/AC used in the present study (Fig. 9), the edge or corner Pd sites which are effective for NH_3 formation will become inactive. Thus the selectivity to N_2 would be enhanced by the addition of Cu.

Skoda *et al.* (29) showed that when γ-Al_2O_3 was first impregnated with a $Pd(NO_3)_2$ solution and reduced by hydrogen, Pd particles of 2 wt% Pd–2.5 wt% Cu/γ-Al_2O_3 were mostly covered with Cu. As a result, this catalyst was inactive for the hydrogenation of toluene. In the present 5 wt% Pd–Cu/AC (Pd/Cu $\leqq$ 3 wt%) catalyst, it is likely that the surface of the Pd particles is nearly covered by Cu (Fig. 9c) at Cu loadings of 1–3 wt%. The decrease in N_2 selectivity (i.e., the increase in NH_3 selectivity) can be explained by an ensemble effect of Cu. In the catalysts with high loadings of Cu, most of the Pd atom will be isolated by the ensemble effect of Cu. The NO_2^- molecules adsorbed on the active Pd are well separated from each other. The hydrogenation of the separated NO_2^- is likely to form NH_3, because of the difficulty of the recombination of N atoms to N_2. In conclusion, N_2 selectivity changes on addition of Cu is caused by the selective poisoning of nonselective sites at low loadings and by the isolation of Pd sites by the ensemble effect of Cu.

ACKNOWLEDGMENT

This work was partly supported by the Steel Industry Foundation for the Advancement of Environmental Protection Technology.

REFERENCES

1. Canter, L. W., "Nitrates in Groundwater." CRC Press, Boca Raton, FL, 1996.
2. Van der Hoek, J. P., Van der Hoek, W. K., and Klapwijk, A., *Water Air Soil Pollut.* **37**, 41 (1988).
3. Schmidt, J., and Vorlop, K. D., *in* "Proceedings, 4th European Congress on Biotechnology," Vol. 1, p. 155. Elsevier, Amsterdam, 1987.
4. Tacke, T., and Vorlop, K. D., *in* "Dechema Biotechnology Conferences," Vol. 3, Part b, p. 1007, VCH, Weinheim, 1989.
5. Hörold, S., Vorlop, K. D., Tacke, T., and Sell, M., *Catal. Today* **17**, 21 (1993).
6. Hörold, S., Tacke, T., and Vorlop, K. D., *Environ. Technol.* **14**, 931 (1993).
7. Pintar, A., Setine, M., and Levec, J., *J. Catal*. **174**, 72 (1998).
8. Pintar, A., Batista, J., and Levec, J., *Water Sci. Technol*. **37**, 177 (1998).
9. Strukul, G., Pinna, F., Marella, M., Meregalli, L., and Tomaselli, M., *Catal. Today* **27**, 209 (1996).
10. Deganello, F., Liotta, L. F., Macaluso, A., Venezia, A. M., and Deganello, G., *Appl. Catal. B* **24**, 265 (2000).
11. Ilinitch, O. M., Nosova, L. V., Gorodetskii, V. V., Ivanov, V. P., Trukhan, S. N., Gribov, E. N., Bogdanov, S. V., and Cuperus, F. P., *J. Mol. Catal. A* **158**, 237 (2000).
12. Prüsse, U., Hahnlein, M., Daum, J., and Vorlop, K. D., *Catal. Today* **55**, 79 (2000).
13. Prüsse, U., Daum, J., Bock, C., and Vorlop, K. D., *Stud. Surf. Sci. Catal*. **130**, 2237 (2000).
14. Prüsse, U., and Vorlop, K. D., *J. Mol. Catal*. **173**, 313 (2001).
15. Strukul, G., Gavagnin, R., Pinna, F., Modaferri, E., Perathoner, S., Centi, G., Marella, M., and Tomaselli, M., *Catal. Today* **55**, 139 (2000).
16. Pintar, A., Batista, J., and Levec, J., *Chem. Eng. Sci*. **56**, 1551 (2001).
17. Pintar, A., Batista, J., and Levec, J., *Catal. Today* **66**, 503 (2001).
18. Vorlop, K. D., and Tacke, T., *Chem.-Ing.-Tech*. **61**, 836 (1989).
19. Matatov-Meytal, Y., Barelko, V., Yuranov, I., Kiwi-Minsker, L., Renken, A., and Sheintuch, M., *Appl. Catal. B* **31**, 233 (2001).
20. Hayashi, H., Uno, M., Kawasaki, S., and Sugiyama, S., *Nippon Kagaku Kaishi* **2000**, 547.
21. Renouprez, A. J., Lebas, K., Bergeret, G., Rousset, J. L., and Delichere, P., *Stud. Surf. Sci. Catal.* **101**, 1105 (1996).
22. JCPDS Alphabetical Index, *Inorg. Phases*, #7-138.
23. Van Langeveld, A. D., Hendrickx, H. A. C. M., and Nieuwenhuys, B. E., *Thin Solid Films* **109**, 179 (1983).
24. Rochefort, A., Abon, M., Delichere, P., and Bertolini, J. C., *Surf. Sci.* **294**, 43 (1993).
25. Hultgren, R., Desai, P. A., Gleiser, M., and Kelly, K. K., *in* "Selected Values of the Thermodynamic Properties of Binary Alloys," p. 777. Am. Soc. Metals, Metal Park, OH, 1973.
26. Massalski, T. B., Okamoto, H., Subramanian, P. R., and Kacprzak, L., *in* "Binary Alloy Phase Diagrams," 2nd ed., p. 1454. ASM International, Materials Park, OH, 1990.
27. Boudart, M., *Adv. Catal.* **20**, 153 (1963).
28. Mélendrez, R., Del Angel, G., Bertin, V., Valenzuela, M. A., and Barbier, J., *J. Mol. Catal. A* **157**, 143 (2000).
29. Skoda, F., Astier, M. P., Pajonk, G. M., and Primet, M., *Catal. Lett*. **29**, 159 (1994).